Journal of Ovonic Research Vol. 6, No. 5, September-October 2010, p. 201 – 210

PHOTONIC BAND STRUCTURE OF QUASI 1D METALLIC SERIAL LOOP STRUCTURE

SANJEEV K SRIVASTA*, U. C. SRIVASTAVA, S. P. OJHA[a]
Dept. of Physics, Amity Institute of Applied Sciences, Amity University, Noida-201301, India
[a]Dept. of Applied Physics, Institute of Technology, Banaras Hindu University, Varanasi-221005, India

In this communication we investigate theoretically the existence of photonic band gaps in a quasi one-dimensional metallic serial loop structure (SLS). This type of structure consists of an infinite number of unit cells in the form of loop joined together with the segment of other material. Serial loop structures show larger band gaps in comparison to star waveguide structure. In order to find the dispersion relation and hence the band gaps interface response theory (IRT) has been applied. Analysis of the dispersion curves shows that metallic SLS (for which segment material is metallic) possess larger band gaps in comparison with the normal metallic photonic crystal structure, for the same values of parameters. Also metallic SLS show large number of forbidden bands than the normal metallic PC structure when the refractive index of the dielectric material increases. In addition to this we study the effect of variation of plasma frequency of metals on the band gaps of metallic SLS. Finally the effect of change in the physical parameters of the loop and segment material on the forbidden frequency band has been investigated.

(Received August 1, 3010; accepted September 19, 2010)

Keywords: Photonic crystal structure, Metallic serial loop structure, Starwaveguide structure, Dispersion, bandgaps

1. Introduction

In the last twenty years Photonic Crystal (PC) structures have been studied extensively and received a great deal of attention due to its perceived applications, peculiar optical properties and new physical phenomena [1-10]. Photonic crystals or photonic band gap materials (PBG) are a new class of optical materials which have the properties to manipulate the flow of electromagnetic waves within it. These are periodic dielectric structures that forbid propagation of electromagnetic waves in a certain frequency range. In the recent past another type of photonic structures, called star waveguide or comb like waveguide structures have been proposed which exhibit large photonic band gaps separated by a narrow transmission bands [11-15]. The star waveguide structure is composed of an infinite one dimensional waveguide called the backbone or substrate along which finite side branches are grafted periodically. The physical characteristics of this star waveguide (SWG) structure are the periodicity, which is the distance between the two sites, the length of each grafted branches and the refractive indices of the constituent materials. In recent past another one-dimensional quasi periodic structure called serial loop structure (SLS) or networked waveguide structure [16-19] has been proposed and investigated. The SLS structure is different from the SWG structure in a way that the resonator is made of a loop rather than a side branches. This type of structure consists of an infinite number of unit cell joined together with the segment of other material. The unit cell is in the form of loop or ring which has two arms, the refractive index and the length of the arms may be same or different. Such types of structures show

* Corresponding author: sanjeev17th@gmail.com

larger forbidden bands in comparison to star waveguide structure. In this communication we propose a metallic loop structure which is of two types: one in which the segment is made of metallic conductor and loop is made of dielectric or semiconductor while in the second case the loop is made of metallic conductor and segment is made of dielectric or semiconductor. We choose metallic structure because metallic photonic structures are light in weight, small in size, cheaper and low in costs. Also, it has better tolerance to temperature fluctuations and is applicable for the application at high temperature above 1000^0C. Dispersion relation of the proposed structure has been found by employing Green' function method. From the analysis of the dispersion curves it is observed that metallic SLS (for which segment material is metallic) possess larger band gaps in comparison with the normal metallic photonic crystal (PC) structure, for the same values of parameters. Also metallic SLS show large number of forbidden bands than the normal metallic PC structure when the refractive index of the dielectric material increases. Further, we study the effect of variation of plasma frequency on the band gaps of metallic SLS. Finally the effect of change in the physical parameters of the loop and segment material on the forbidden frequency band has been investigated.

2. Theoretical model

The schematic representation of serial loop structure is depicted in the Fig (1). The unit cell of SLS consist the two arms of length ($b_1 + b_2$), pasted together with segment of length '*a*' and refractive index n_1. For the present study we consider that the two arms of the loop have the same length (i.e. $b_1 = b_2 = b$) as well as the same refractive ($n_2 = n_3 = n_2$). The dispersion relation, at normal incidence angle, of serial loop structure can be obtained by using the Green's function method [17-19] and is given by

$$\cos(Kd) = \cos\left(\frac{n_1 \omega a}{c}\right)\cos\left(\frac{n_2 \omega b}{c}\right) - \left(\frac{n_1^2 + 4n_2^2}{4n_1 n_2}\right)\sin\left(\frac{n_1 \omega a}{c}\right)\sin\left(\frac{n_2 \omega b}{c}\right) \quad (1)$$

Here '*K*' is propagation vector along the direction of waveguide, n_1 and n_2 are the refractive indices of the loop and segment materials, ω is angular frequency '*c*' is the velocity of light, $d = a + 2b$

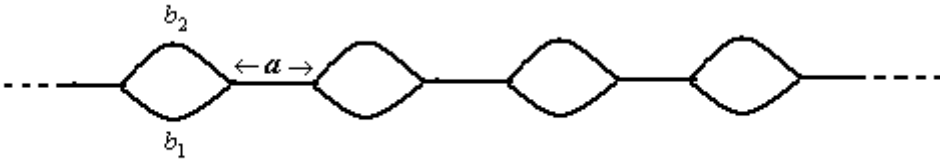

Fig. (1) ←unit cell →

Fig. 1. Schematic representation of serial loop structure (SLS).

The expression for the dispersion relation of normal PC structure at normal incidence angle, obtained by transfer matrix method can be written as [20]

$$\cos(Kd) = \cos\left(\frac{n_1 \omega a}{c}\right)\cos\left(\frac{n_2 \omega b}{c}\right) - \left(\frac{n_1^2 + n_2^2}{2n_1 n_2}\right)\sin\left(\frac{n_1 \omega a}{c}\right)\sin\left(\frac{n_2 \omega b}{c}\right) \quad (2)$$

In this expression n_1 and n_2 are the refractive indices of the alternate layers of PC structure, *a* and *b* are their widths and $d = a + b$ is the lattice constant. Since for metals refractive index is complex and depends on frequency. Hence we will use the frequency-dependent dielectric function for the metals governed by Drude model [21]. This model gives the best fit to the measured data over a wide range of frequency, and is defined as

$$n(\omega) = \sqrt{\varepsilon(\omega)} = \left(1 - \frac{\omega_p^2}{(\omega + i\gamma)\omega}\right)^{1/2} = n_r + in_i \tag{3}$$

Where ω_p is the plasma frequency of the conduction electron and γ is the damping frequency related to the absorption the conducting materials. Also for the metals propagation vector *K* is complex and can be written as $K = K_r + iK_i$. On substituting the value of Eq.(3) into Eqs. (1) and (2), we can obtain the expression for the dispersion relation of the proposed metallic structures. Hence the dispersion relation for the metallic SLS in which loop is metallic is given by

$$\begin{aligned} cos(K(\omega)d) &= cos(K_r(\omega)d + iK_i(\omega)d) \\ &= P - QR - ST + i(QT - U - SR) \end{aligned} \tag{4}$$

for the metallic SLS in which segment is metallic, is given by

$$\begin{aligned} cos(K(\omega)d) &= cos(K_r(\omega)d + iK_i(\omega)d) \\ &= P' - Q'R' + S'T' - i(Q'T' + U' + S'R') \end{aligned} \tag{5}$$

And finally for metallic PC structure the dispersion relation is given by

$$\begin{aligned} cos(K(\omega)d) &= cos(K_r(\omega)d + iK_i(\omega)d) \\ &= P' - Q'X + S'Y - i(Q'Y + U' + S'X) \end{aligned} \tag{6}$$

The abbreviations of the symbols *P*, *Q*, *R*, *S*, *T*, *U*, *P'*, *Q'*, *R'*, *S'*, *T' U'*, *X* and *Y* are as follows

$$P = cos\left(\frac{n_1\omega a}{c}\right)cos\left(\frac{n_r\omega b}{c}\right)cosh\left(\frac{n_i\omega b}{c}\right); \quad Q = sin\left(\frac{n_1\omega a}{c}\right)sin\left(\frac{n_r\omega b}{c}\right)cosh\left(\frac{n_i\omega b}{c}\right)$$

$$R = \left(\frac{n_r}{4n_1}\right)\left(\frac{n_1^2 + 4(n_r^2 + n_i^2)}{(n_r^2 + n_i^2)}\right); \quad S = sin\left(\frac{n_1\omega a}{c}\right)cos\left(\frac{n_r\omega b}{c}\right)sinh\left(\frac{n_i\omega b}{c}\right);$$

$$T = \left(\frac{n_i}{n_1}\right)\left(\frac{n_1^2 - 4(n_r^2 + n_i^2)}{(n_r^2 + n_i^2)}\right); \quad U = cos\left(\frac{n_1\omega a}{c}\right)sin\left(\frac{n_r\omega b}{c}\right)sinh\left(\frac{n_i\omega b}{c}\right);$$

$$P' = cos\left(\frac{n_r\omega a}{c}\right)cos\left(\frac{n_2\omega b}{c}\right)cosh\left(\frac{n_i\omega a}{c}\right); \quad Q' = sin\left(\frac{n_r\omega a}{c}\right)sin\left(\frac{n_2\omega b}{c}\right)cosh\left(\frac{n_i\omega a}{c}\right)$$

$$R' = \left(\frac{n_r}{4n_2}\right)\left(\frac{4n_2 + (n_r^2 + n_i^2)}{(n_r^2 + n_i^2)}\right); S' = cos\left(\frac{n_r\omega a}{c}\right)sin\left(\frac{n_2\omega b}{c}\right)sinh\left(\frac{n_i\omega a}{c}\right);$$

$$U' = sin\left(\frac{n_r\omega a}{c}\right)cos\left(\frac{n_2\omega b}{c}\right)sinh\left(\frac{n_i\omega a}{c}\right); \quad T' = \left(\frac{n_i}{4n_2}\right)\left(\frac{(n_r^2 + n_i^2) - 4n_2}{(n_r^2 + n_i^2)}\right)$$

$$X = \left(\frac{1}{2}\right)\left(\frac{n_2 n_r + n_r(n_r^2 + n_i^2)}{n_2(n_r^2 + n_i^2)}\right); \quad Y = \left(\frac{1}{2}\right)\left(\frac{n_i(n_r^2 + n_i^2) - n_2 n_r}{n_2(n_r^2 + n_i^2)}\right)$$

If $f_1(\omega)$ and $f_2(\omega)$ represents the real and imaginary parts of $cos(K(\omega)d)$ then Eqs. (4), (5) and (6) can be written as

$$f_1(\omega)+if_2(\omega) = P-QR-ST+i(QT-U-SR) \tag{7}$$

$$f_1(\omega)+if_2(\omega) = P^{'}-Q^{'}R^{'}+S^{'}T^{'}-i\left(Q^{'}T^{'}+U^{'}+S^{'}R^{'}\right) \tag{8}$$

$$f_1(\omega)+if_2(\omega) = P^{'}-Q^{'}X+S^{'}Y-i\left(Q^{'}Y+U^{'}+S^{'}X\right) \tag{9}$$

Now comparing the real and imaginary parts of both sides of Eqs. (7), (8) and (9), we can write $f_1(\omega)$ and $f_2(\omega)$ explicitly in the forms as

$$\cos(K_r(\omega)d) = f_1(\omega) = P-QR-ST \tag{7a}$$

$$\cos(K_i(\omega)d) = f_2(\omega) = QT-U-SR \tag{7b}$$

$$\cos(K_r(\omega)d) = f_1(\omega) = P^{'}-Q^{'}R^{'}+S^{'}T^{'} \tag{8a}$$

$$\cos(K_i(\omega)d) = f_2(\omega) = Q'T'+U'+S'R' \tag{8b}$$

$$\cos(K_r(\omega)d) = f_1(\omega) = P^{'}-Q^{'}X+S^{'}Y \tag{9a}$$

$$\cos(K_i(\omega)d) = f_2(\omega) = Q'Y+U'+S'X \tag{9b}$$

We are interested only the real parts of the above Eqs. i.e in Eqs (7a), (8a) and (9a) because only this part of the equations show the real propagation of EM waves through the structure. In the next section we will compute, numerically, the band structure with the help of Eqs. (7a). (8a) and (9a), for different values of the plasma frequency, absorption of metals, refractive indices and lengths of the constituent materials.

3. Results and discussion

For the sake of numerical computations we choose $\omega_p = 1.5x10^{16}$ Hz, d= 8x10^{-8}m, $\gamma = 0.1\omega_p$, a=b=0.5d,. The frequency range of forbidden bands can be seen from the dispersion curves plotted between $K_r(\omega)d$ Vs normalized frequency $\left(\omega d/2\pi c\right)$ as well as with the cosine curve plotted between $f_1(\omega)$ Vs normalized frequency $\left(\omega d/2\pi c\right)$. Since the maximum and minimum value of cosine is +1 and -1, therefore the portion of the curves which lies within this limit gives allowed bands and which lies above these values give the forbidden or reflection bands. Figs 2(a), 2(c); 3(a), 3(c) and 4(a), 4(c) show the dispersion curves of the loop structure for which n_1 is metallic and $n_2 = 1.35$, 2.3 and 3.5 while Figs. 2(b),2(d); 3(b), 3(d) and 4(a), 4(d) show the dispersion curves of the loop structure, for which n_2 is metallic and $n_1 = 1.35$, 2.3 and 3.5 respectively. From the study of these figures, it is found that the number of bands in both cases is same whether the loop is metallic or segment is metallic. Further, when the refractive index of the loop (or segment) material is increased the number of bands also increases. The number bands are 3, 5 and 7 when we take $n_2 = 1.35$, 2.3 and 3.5 for metallic loop and the same number of bands is found for metallic segment where we take $n_1 = 1.35$, 2.3 and 3.5 respectively. It is interesting to note that the loop structure for which segment material having refractive index (n_1) is metallic show wider reflection bands in comparison to the loop structure where loop is metallic. Also, it has been found that the band gets enlarged when the refractive index of other constituent material increases by taking one constituent material as metal either loop or segment. Dispersion curves for metallic PC structure where we take n_1 as metallic layer and $n_2 = 1.35$, 2.3 and 3.5 have been illustrated in Figs. 5(a)-(f). Comparing the band structure of metallic PC with those of Figs. 2(a)-4(d), we observe that metallic loop structure in which segment is metallic posses larger band gaps than that of metallic PC structure for the same refractive index contrast and length parameters. At the same time width of the reflection bands for the loop structure where loop is metallic smaller. From these results we may conclude that the metallic SLS (where n_1 is metallic) has wider as well

as larger number of photonic band gaps than the metallic PC structure The range of forbidden frequency bands for the metallic segment, metallic loop serial loop and metallic PC structures in the unit of $\left(\omega d/2\pi c\right)$ has been reported in the Table (1).

Table 1. Range of forbidden frequency bands for $\omega_p = 1.5x10^{16}$ *Hz, d= 8x10*$^{-8}$*m, a = b = 0.5d,* $\gamma = 0.1\omega_p$.

For segment metallic structure i.e. n_1 metallic			For loop metallic structure i.e. n_2 metallic			For metallic PC structure i.e. n_1 metallic		
n_2	Forbidden bands in $\left(\omega d/2\pi c\right)$	Bandwidth in $\left(\omega d/2\pi c\right)$	n_1	Forbidden bands in $\left(\omega d/2\pi c\right)$	Bandwidth in $\left(\omega d/2\pi c\right)$	n_2	Forbidden bands in $\left(\omega d/2\pi c\right)$	Bandwidth in $\left(\omega d/2\pi c\right)$
1.35	0.375 — 0.703 0.856 — 1.036 1.262 — 1.415	0.328 0.180 0.153	1.35	0.533 – 0.683 0.898 – 1.013 1.290 – 1.399	0.150 0.115 0.109	1.35	0.463 – 0.689 0.912 – 0.988 1.297 – 1.388	0.226 0.076 0.091
2.3	0.347 — 0.505 0.579 — 0.794 0.921 — 1.035 1.213 — 1.303 1.486 — 1.618	0.258 0.215 0.114 0.090 0.132	2.3	0.326 – 0.539 0.636 – 0.773 0.934 – 1.022 1.221 – 1.303 1.513 – 1.597	0.213 0.137 0.088 0.082 0.084	2.3	0.292 – 0.534 0.647 – 0.754 1.224 – 1.304	0.242 0.107 0.080
3.5	0.171 — 0.367 0.407 — 0.592 0.653 — 0.802 0.896 — 0.990 1.121 — 1.179 1.322 — 1.403 1.537 — 1.628	0.196 0. 149 0.185 0.094 0.058 0.081 0.091	3.5	0.218 – 0.392 0.435 – 0.595 0.662 – 0.801 0.896 – 0.992 1.122 – 1.181 1.321 – 1404 1.533 – 1.633	0.174 0.161 0.139 0.096 0.059 0.083 0.100	3.5	0.198 – 0.392 0.442 – 0.603 0.709 – 0.762 1.118 – 1.182	0.194 0.161 0.053 0.064

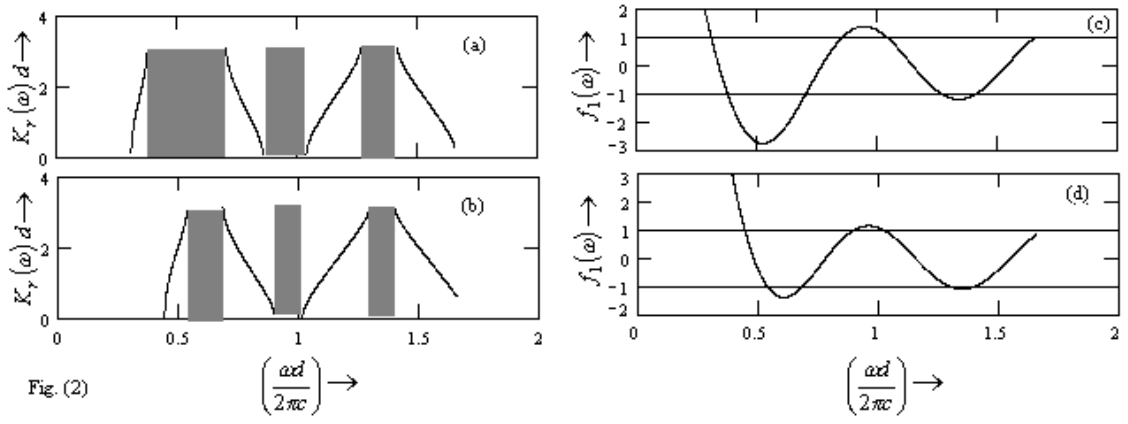

Fig. 2. Dispersion and cosine curves of SLS for (a) &(c) metallic segment i.e. n_1 *metallic and* n_2 *= 1.35 and (b) & (d) metallic loop i.e.* n_2 *metallic and* n_1 *= 1.35 and other parameters are* $\omega_p = 1.5x10^{16}$ *Hz, d= 8x10*$^{-8}$*m, a = b = 0.5d,* $\gamma = 0.1\omega_p$.

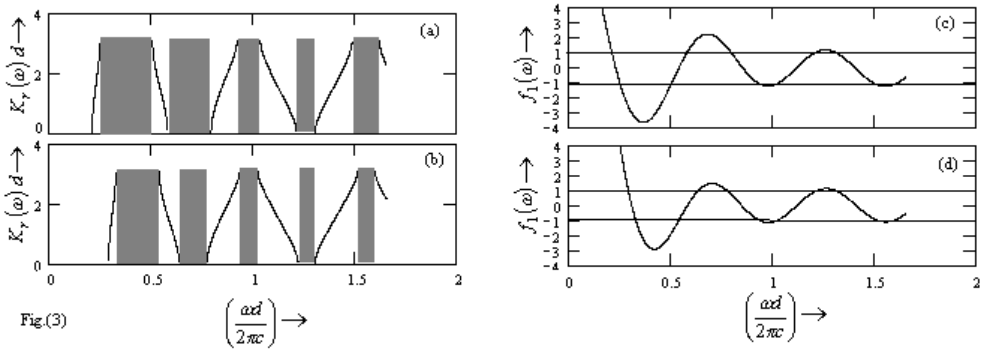

Fig. 3. Dispersion and cosine curves of SLS for (a) &(c) metallic segment i.e. n_1 metallic and $n_2 = 2.3$ and (b) & (d) metallic loop i.e. n_2 metallic and $n_1 = 2.3$ and other parameters are $\omega_p = 1.5x10^{16}$ Hz, $d = 8x10^{-8}$m, $a = b = 0.5d$, $\gamma = 0.1\omega_p$.

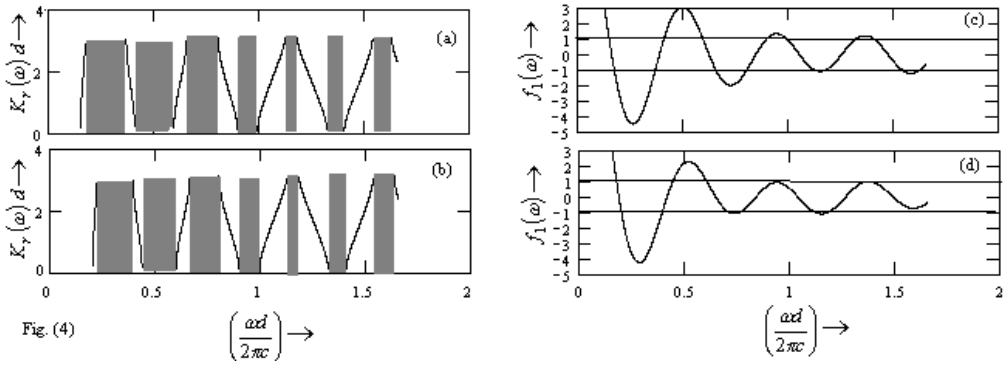

Fig. 4. Dispersion and cosine curves of SLS for (a) &(c) metallic segment i.e. n_1 metallic and $n_2 = 3.5$ and (b) & (d) metallic loop i.e. n_2 metallic and $n_1 = 3.5$ and other parameters are $\omega_p = 1.5x10^{16}$ Hz, $d = 8x10^{-8}$m, $a = b = 0.5d$, $\gamma = 0.1\omega_p$.

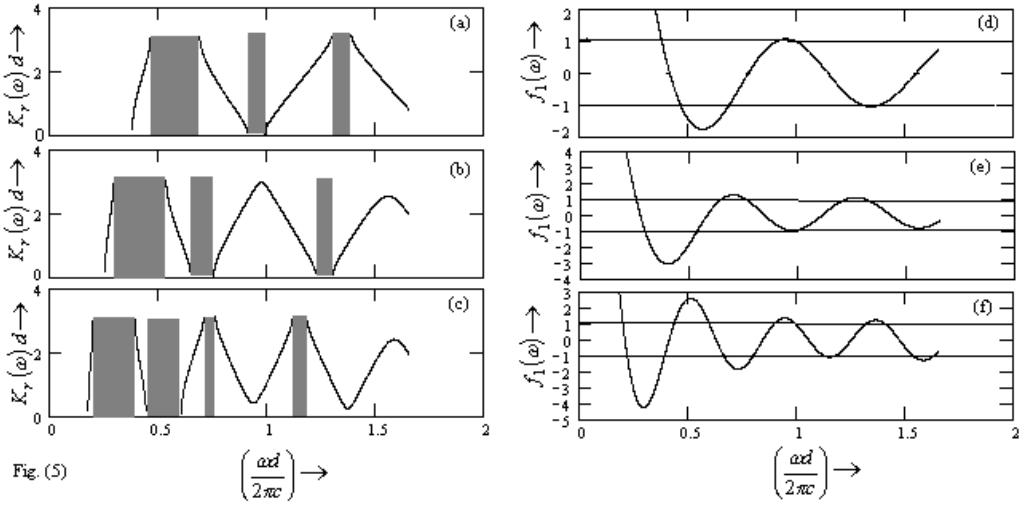

Fig. 5. Dispersion and cosine curves of metallic PC structure (a) &(d) n_1 metallic and $n_2 = 1.35$ and (b) & (e) n_1 metallic and $n_2 = 2.3$ and (c) & (f) n_1 metallic and $n_2 = 2.3$ and other parameters are $\omega_p = 1.5x10^{16}$ Hz, $d = 8x10^{-8}$m, $a = b = 0.5d$, $\gamma = 0.1\omega_p$.

The effect of plasma frequency on the reflection bands of the proposed structures can be seen from the Figs. 2(a)-(b) and Figs. 6(a)-(d). The dispersion curves are plotted for different values of plasma frequency, viz. ω_p =1.5x10^{16}, 2x10^{16} and 2.5x10^{16} Hz respectively. The other parameters are taken as $a = b$ =0.5d, γ =0.1 ω_p and n_1 =1.35 for metallic loop and n_2 =1.35 for metallic segment SLS. Analysis of the band structure shows that when the plasma frequency of metallic component increases width of the reflection bands also increases in both cases. Width of the forbidden bands becomes narrower and narrower as one move towards the higher frequency sides. Further, we see that the number of reflection bands are same for different values of ω_p but there position changes. Thus the variation in plasma frequency doesn't change the number of bands but it increases the bandwidth as well as the position of the reflection bands. Moreover, there is a very slight change in the width of the forbidden bands lying at the higher frequency side, viz. the width of forbidden band changes from 0.170 to 0.171 $\left(\omega d/2\pi c\right)$when ω_p changes from 2x10^{15}Hz to 2.5x10^{15} Hz for metallic segment SLS and 0.124 to 0.132 $\left(\omega d/2\pi c\right)$for metallic loop SLS, reported in Table (2). Figs. 7(a)-(d) show the dispersion curves for the different length ratio of loop and segment material. For this we choose a = 0.6d; b = 0.4d and in the second case a= 0.4d; b= 0.6d respectively, and other parameters are same as taken previously. From the study of Figs. 7(a)-(b), we observe that when the length of the metallic segment is large then the width of second and third bands increases while it is slightly smaller for the first band. But when we reverse the length ratio of the materials, then width of first and third forbidden bands are increased but the width of second bands decreases. Further, it is interesting to see that the metallic SLS in which loop is metallic and have length ratio as a= 0.4d; b= 0.6d show wider reflection bands than metallic SLS in which segment is metallic for the same length ratio. From these investigations, it can be inferred that by increasing the lengths of metallic loop the width of reflection bands can be enhanced in comparison to metallic segment SLS. Further, the reflection bands can be tuned to over a wider range of frequency by changing the lengths of either segment or loop material and the effect is more significant in case of metallic SLS in which segment is metallic, the range and width of the forbidden bands are shown in the Table (3).

Table 2. Range of forbidden frequency bands for $\gamma = 0.1\omega_p$, d= 8x10^{-8}m, a = b = 0.5d, and n_1 = 1.35 for n_2 metallic and n_2 =1.35 for n_1 metallic.

For segment metallic structure i.e. n_1 metallic			For loop metallic structure i.e. n_2 metallic	
Plasma Frequency $\left(\omega_p\right)$	Forbidden bands in $\left(\omega d/2\pi c\right)$	Bandwidth in $\left(\omega d/2\pi c\right)$	Forbidden bands in $\left(\omega d/2\pi c\right)$	Bandwidth in $\left(\omega d/2\pi c\right)$
1.5 x 10^{16} Hz	0.375 — 0.703 0.856 — 1.036 1.262 — 1.415	0.328 0.180 0.153	0.533 – 0.683 0.898 – 1.013 1.290 – 1.399	0.150 0.115 0.109
2.0 x 10^{16} Hz	0.407 – 0.804 0.894 – 1.135 1.304 – 1.474	0.397 0.241 0.170	0.596—0.839 0.978 – 1.102 1.324 – 1.472	0.270 0.124 0.148
2.5 x 10^{16} Hz	0.439 – 0.895 0.941 – 1.252 1.371 – 1.542	0.456 0.311 0.171	0.599 – 0.992 1.078 – 1.210 1.375 – 1.559	0.393 0.132 0.184

Table 3. Range of forbidden frequency bands for $\omega_p = 1.5x10^{16}$, $\gamma = 0.1\omega_p$, *d= 8x10*$^{-8}$*m, and* n_1 *= 1.35 for* n_2 *metallic and* n_2 *=1.35 for* n_1 *metallic .*

For segment metallic structure i.e. n_1 metallic			For loop metallic structure i.e. n_2 metallic	
Length parameters	Forbidden bands in $\left(\omega d/2\pi c\right)$	Bandwidth in $\left(\omega d/2\pi c\right)$	Forbidden bands in $\left(\omega d/2\pi c\right)$	Bandwidth in $\left(\omega d/2\pi c\right)$
a = 0.6*d*; b = 0.4*d*	0.413 – 0.764 0.926 – 1.053 1.276 – 1.504	0.351 0.127 0.288	0.484 – 0.644 0.874 – 0.954 1.249 – 1.340	0.160 0.080 0.090
a= 0.4*d*; *b*= 0.6*d*	0.407 – 0.804 0.894 – 1.135 1.304 – 1.474	0.397 0.241 0.170	0.350 – 0.633 0.784 – 1.014 1.248 – 1.340	0.283 0.229 0.092

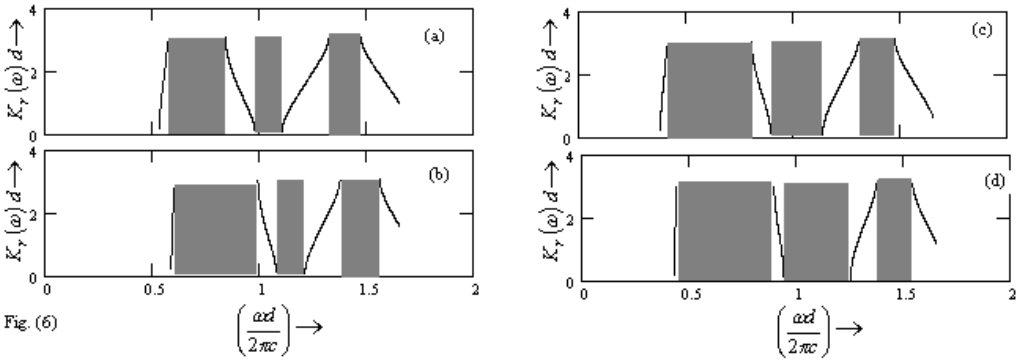

Fig. (6)

Fig. 6. Dispersion curves of SLS for (a) n_2 *metallic and* n_1 *= 1.35,* $\omega_p = 2.0x10^{16}$ *Hz (b)* n_2 *metallic and* n_1 *= 1.35,* $\omega_p = 2.5x10^{16}$ *Hz (c)* n_1 *metallic and* n_2 *= 1.35,* $\omega_p = 2.0x10^{16}$ *Hz and (d)* n_1 *metallic and* n_2 *= 1.35,* $\omega_p = 2.5x10^{16}$ *Hz and other parameters are a = b = 0.5d, .* $\gamma = 0.1\omega_p$

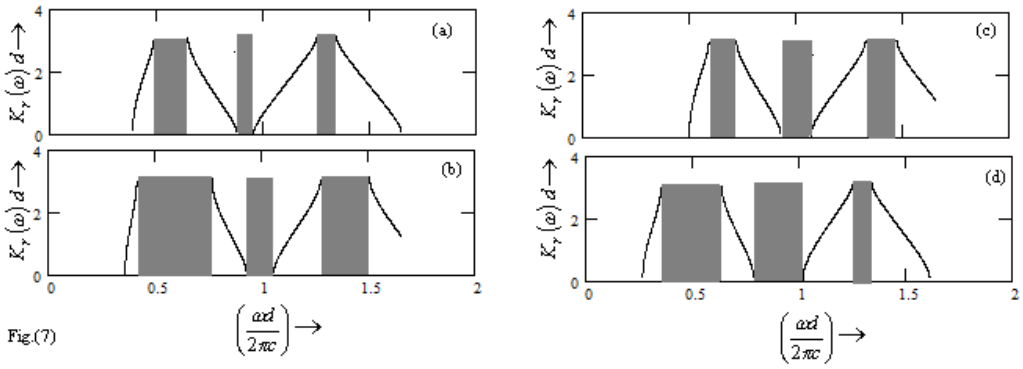

Fig.(7)

Fig. 7. Dispersion curves of SLS for (a) n_2 metallic and n_1 = 1.35, a = 0.6d ; b = 0.4d (b) n_1 metallic and n_2 = 1.35, a = 0.6d ; b = 0.4d (c) n_2 metallic and n_1 = 1.35, a = 0.4d ; b = 0.6d and (d) n_1 metallic and n_2 = 1.35, a = 0.6d ; b = 0.4d and other parameters are $\omega_p = 1.5x10^{16}$ Hz, d= $8x10^{-8}$m, $\gamma = 0.1\omega_p$.

4. Conclusions

In conclusion, we have investigated theoretically a different type of wave guide structure called metallic SLS. In the proposed structure considered here in the two forms one in which segment material of structure is made of metal and other in which loop is metallic. From the analysis of the dispersion curves it is found that metallic SLS in which segment is metallic show wider frequency bands in comparison with the metallic SLS in which loop is metallic and metallic PC structure for the same physical and materials parameters. From this study it is concluded that band gap can be enlarged by using the metallic segment in the metallic SLS. Further the study of change of plasma frequency on reflection bands shows that variation in plasma frequency doesn't change the number of bands but it increases the bandwidth and the position of the reflection bands. Therefore, in conclusion it can be say that the range and width of reflection bands can be tuned to different value by changing the plasma frequency keeping other parameters constant. The proposed metallic SLS can be used to design the optical filters, optical reflectors and wavelength multiplexing etc in any region of EM spectrum by the proper selection of material and physical parameters. The metallic SLS have potential applications in the field of optoelectronics and photonics due to the ease in manufacturing technique (lithography) and geometrical constructions.

Acknowledgements

Dr. Sanjeev K Srivastava wishes to thank Amity Institute of Applied Sciences, Amity University, Noida, India, for the necessary facility for this work.

References

[1] E Yablonovitch, Phys. Rev. Lett., **58**, 2059, (1987).
[2] J D Joannopoulos, P. Villeneuve, S Fan, Nature. **386**, 143, (1997).
[3] Yuan K, X Zhen, C-L Li and W L She, Phys. Rev. E , **71**, 1, (2005).
[4] S K Srivastava and S P Ojha, Progress in electromagnetic research, PIER **68**, 91,(2007).
[5] F. Y. Wang, G. X. Li, H. L. Tam, K. W. Cheah, and S. N. Zhu, Appl. Phys. Lett., **92**, 211109 (2008).
[6] V. A. Tolmachev and T. S. Perova, Opt. & Spectroscopy **101**, 791, (2006).
[7] Yonggang Wu, Zhanshan Wang, Mu Gu, Li Wang, Xiaoyan Lin, Lingyan Chen, and Rongkun Xu , Appl. Phys. Lett. **85**, 4337, (2004).

[8] Jin-Hui Wu , A. Raczyski J. Zaremba S. Zieliska-Kaniasty; M. Artoni G. C. La Rocca, J. Mod. Opt., **56,** 768, 2009.
[9] D. Owens, C. F.-Hernandez, B. Kippelen, Thin Solid Films **517**, 2736 (2009).
[10] X. Hu , Z. Liu, and Q. Gong, Phys. Lett. A **372** 333, (2008).
[11] Dobrzynski, L., A. Akjouj, A. Djafari-Rouhani, J. O. Vasseur, and J. Zemmouri, Phys. Rev. B, **57**, R9388, (1998).
[12] Vasseur, J. O., P. A. Deymier, L. Dobrzynski, B. Djafari-Rouhani, and A. Akjouj, Phys .Rev. B, **55**, 10434, (1997).
[13] Srivastava, S. K. and S. P. Ojha, Progress In Electromagnetic Research, PIER **68**, 91, (2007).
[14] L. Zhang, Z. Wang, L. Chen, H. Li and Y. Zhang, Opt. Comm. **281**, 3681, (2008).
[15] Srivastava, S. K. and S. P. Ojha, Progress In Electromagnetic Research M, PIERM **9,** 21, (2009).
[16] Mir, A., A. Akjouj, J. O. Vasseur, B. Djafari-Rouhani, N. Fettouhi, E. Boudouti, L. Dobrzynski, J. Zemmouri, J. Phys. Condense. Matter, **15,** 1593 (2003).
[17] E. H. El Boudouti, N. Fettouhi, A. Akjouj, B. Djafari-Rouhani, A. Mir, J. O. Vasseur, L. Dobrzynski, and J. Zemmouri , J. Appl. Physics **95**, 1102 (2004).
[18] J.O Vasseur, A. Akjouj, L Dobrzyski, B. Djafari-Rouhani and E. H. El Boudouti, Sruf. Sci. Rep. **54**, 1 (2004).
[19] W. Tan, Z.G. Wang, H. Chen, Phys. Rev. E, **77**, 026603-1 (2008).
[20] P. Yeh. Optical waves in layered media. New York: Wiley, 1988.
[21] M A Ordal, L L Long, R J Bell, S E Bell, R R Bell, R W Alexander Jr, C A Ward, Applied Optics, **22**, 1099 (1983).